

## STRUCTURE INVERSIONS WITH THE VIRGO DATA

THIERRY APPOURCHAUX

*Space Science Department  
ESTEC, NL-2200 AG Noordwijk, The Netherlands*

TAKASHI SEKII

*Institute of Astronomy, University of Cambridge  
Cambridge CB3 0HA, UK*

DOUGLAS GOUGH

*Institute of Astronomy, University of Cambridge  
Cambridge CB3 0HA, UK*

*and*

*Department of Applied Mathematics and Theoretical Physics  
University of Cambridge, Cambridge CB3 9EW, UK*

UMIN LEE

*Astronomical Institute, Tohoku University  
Sendai, Miyagi 980, Japan*

CHRISTOPH WEHRLI

*Physikalisch-Meteorologisches Observatorium Davos  
World Radiation Center, CH-7260 Davos Dorf, Switzerland*

AND

THE VIRGO TEAM

**Abstract.** The p-mode frequencies obtained by the VIRGO instrument have been inverted to derive the solar core structure. Two sets of frequencies have been used in the inversions. The sets are derived from different time series (the second containing the first), using different procedures for fitting the spectra. The influence of the correlations between the p-mode frequencies has been implemented in the inversion procedure. The two data sets are in good agreement with each other, and show no evidence that the sun is significantly different from the latest available standard solar model.

## 1. Introduction

The VIRGO (Variability of solar IRradiance and Gravity Oscillations) investigation on board SOHO (Solar and Heliospheric Observatory) aims at determining the characteristics of pressure and internal gravity oscillations by observing irradiance and radiance variations.

VIRGO contains two different active-cavity radiometers for monitoring the solar 'constant', two three-channel sunphotometers and a low-resolution imager (Luminosity Oscillation Imager, LOI) with 12 'scientific' and 4 guiding pixels, for measuring the radiance distribution over the solar disk at 500 nm. The instrumentation has been described in detail by Fröhlich *et al.*, 1996, and the observed in-flight performance by Fröhlich *et al.*, 1997 (also in these proceedings). Discussion of the performance of the LOI is provided by Appourchaux *et al.*, 1997. Here we report on the result of inversions carried out using the data from the LOI.

## 2. P-mode analysis

After the production of the LOI level-1 data, the 12 scientific pixels are ready to be used for extracting the p modes. The times series from each pixel is detrended using a triangular smoothing with a full width of 1 day, and then the residuals are converted to relative values. For extracting a given degree, the 12 pixels are combined using optimal filters derived by Appourchaux & Andersen, 1990. Since these filters are complex they allow each  $m$  to be separated in an  $l, n$  multiplet. These filters have been successfully used by Appourchaux *et al.*, 1995b,c and by Rabello-Soares *et al.*, 1996. The optimal filters were changed weekly to account for the change in the real size of the solar image (calibrated in flight) and the orientation of the Sun (only the  $B$  angle as  $P$  is maintained zero by the spacecraft orientation).

The spectra obtained have been utilized to derive the p-mode parameters. We use two sets of frequencies for the inversion. Each set was derived from different time series using different fitting procedures. We now describe how the two sets were obtained.

### 2.1. SET A

This is the same set as the set that was presented by Fröhlich *et al.*, 1997. The times series starts on 27 March 1996 and ends on 10 August 1996. The resolution is 84 nHz.

A given  $(m, \nu)$  diagram is fitted using the maximum-likelihood method as described by Appourchaux *et al.*, 1995b. As outlined in that paper, the different  $2l+1$  components spectrum of a given  $l, n$  multiplet are correlated

with each other because of the imperfect isolation of the modes (see also Rabello-Soares, 1996). This additional complication is taken into account in the fitting of the spectra, higher-degree modes leaking into the lower-degree modes, and *vice versa*. For example, in the  $l = 1$  signal we can detect  $l = 6$  and *vice versa*; the  $l = 4$  signal is contaminated by  $l = 7$  (Fig. 1) and *vice versa*, the  $l = 5$  by  $l = 8$  and *vice versa*. The full leakage between the  $2l + 1$  modes of a multiplet and between mode of the higher (or lower) degree has been computed using the computed optimal filters in a manner similar to that of Rabello-Soares, 1996. This is an improvement of the procedure adopted by Appourchaux *et al.*, 1995b, who regarded the mode leakage matrix not to be known a priori and fitted it to the data. The amplitudes of all the modes in the spectrum, together with the frequencies of the target and leaked modes, were fitted simultaneously. The frequencies of the unwanted leaked modes were sometimes fixed using the frequencies obtained from BBSO. This simplification did not influence the frequencies of the target modes substantially, yet it increased the rate of convergence of the iterations in the fitting. In this way the bias on the frequency estimates due to spatial mode leakage was reduced. A total of 92 modes with  $0 \leq l \leq 7$  were obtained in the frequency range  $2.1 \text{ mHz} \leq \nu \leq 3.8 \text{ mHz}$ .

## 2.2. SET B

This is a data set from a longer time series using a different fitting strategy. The times series starts on 27 March 1996 and ends on 5 October 1996. The resolution is 60 nHz.

For  $l \leq 3$  the correlation matrix between the  $2l + 1$  components of a multiplet is used not to fit the power spectra, but the Fourier spectra, as described by Schou, 1992. We did not implement this fitting into the Fourier spectra for  $l \geq 4$ , because of the many more correlations between the various  $l, n$  and  $l', n'$ . Instead we fitted simultaneously both power spectra of the  $l = 1$  and  $l = 6$ , of the  $l = 4$  and  $l = 7$ , and of the  $l = 5$  and  $l = 8$ , taking into account the leakage of the modes. This improved the consistency of the fitted frequencies. The estimate of the  $l = 1$  frequencies given by this fit was not used; instead we used the value obtained from the simultaneous fitting of all the modes with  $l \leq 3$ . The correlation between the uncertainties in the frequencies was retained for use in the inversion. A total of 100 modes with  $0 \leq l \leq 8$  were obtained in the frequency range  $2.1 \text{ mHz} \leq \nu \leq 3.8 \text{ mHz}$ .

## 3. Inversions of the VIRGO frequencies

P-mode frequencies from the two sets have been inverted to investigate the structure of the solar core. The mode with the shallowest inner turning

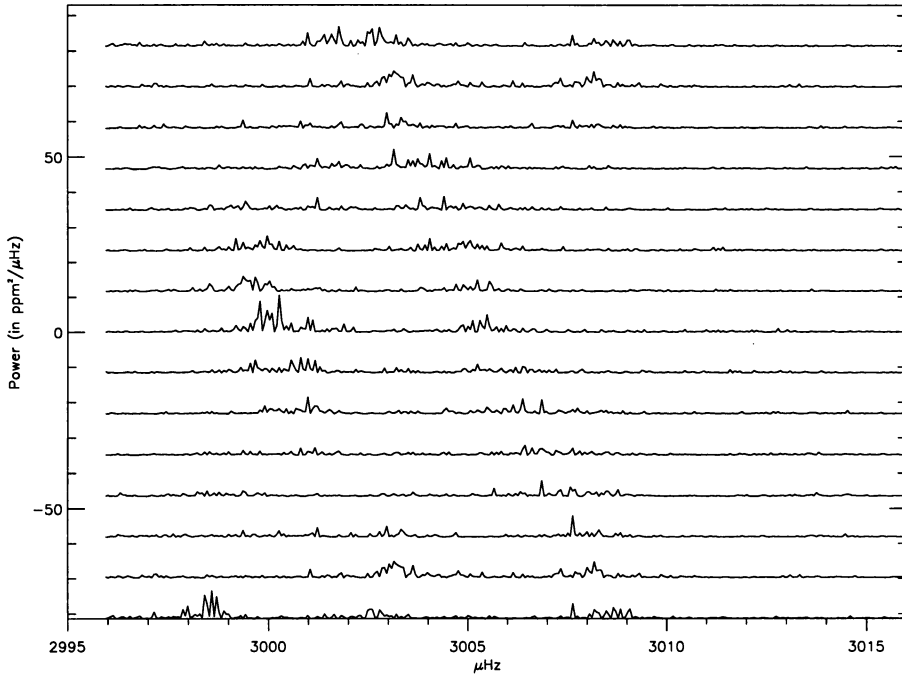


Figure 1. The  $m, \nu$  diagram for the  $l = 7, n = 18$  multiplet from the times series of set B;  $m = -7$  is at the top. It shows an example of the effect of the leakage of the  $l=4, n=19$  into the  $l=7$ . We see clearly the splitting of the  $l=7$  mode and also the effect of the leakage of unwanted modes with different values of  $m$ . The splitting of the  $l = 4$  is not visible because the leakage is more complex: the  $l = 4, m = +4$  mode is partially transmitted by the filter for  $l = 7, m = -7$ , and the  $l = 4, m = -4$  is transmitted by the  $l = 7, m = +7$ .

point penetrates to  $r/R_{\odot} \simeq 0.3$ , and our investigation concentrates on the layers below these depths, since outside these regions the datasets do not provide much information about the solar structure.

The standard strategy of linearization was adopted (e.g., Gough, 1996): we use a theoretical model of the sun as a reference, and then consider the difference between the sun and the model. We attempt to determine how the sun differs from the reference model by considering the difference between the observed frequencies and those of the reference model. The relative frequency difference is equated to a linear functional of the difference in structures:

$$\frac{\delta \nu_i}{\nu_i} \equiv \frac{\nu_{obs,i} - \nu_i}{\nu_i} = \int \left[ K_{u,\gamma_1}^i(r) \frac{\delta u}{u} + K_{\gamma_1,u}^i(r) \frac{\delta \gamma_1}{\gamma_1} \right] dr + \frac{F(\nu_i)}{I_i}, \quad (1)$$

where  $\nu_i$  and  $\nu_{obs,i}$  are respectively the frequency of the model and the observed frequency of the mode  $i$ ; also  $K_{u,\gamma_1}^i$  and  $K_{\gamma_1,u}^i$  are the kernels for

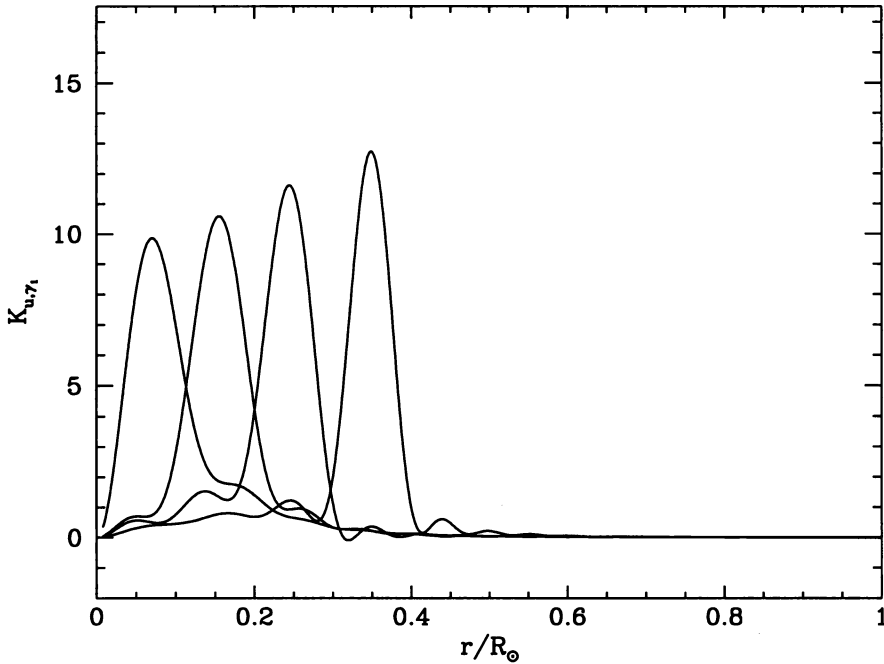
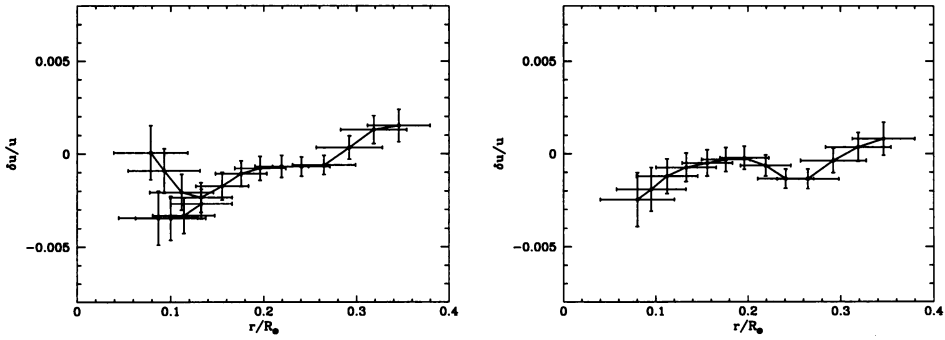


Figure 2. Averaging kernels for the squared isothermal sound speed  $u$  obtained from 1105 combined LOI+LOWL frequencies from set A.

the squared isothermal sound speed  $u$  and the adiabatic exponent  $\gamma_1$ , which are our choice of inversion variables. The two functions  $\delta u$  and  $\delta \gamma_1$  are the differences between the values of  $u$  and the values of  $\gamma_1$  in the sun and in the model. We present below inversions for  $\delta u$ . The term  $F(\nu_i)/I_i$ , where  $F(\nu_i)$  is an arbitrary function of frequency (which we represent as an expansion in terms of Legendre polynomials) and  $I_i$  is the mode inertia (normalization is such that the rms vertical component of the displacement eigenfunction is unity at the surface), is added to represent all the uncertainties that arise from our lack of knowledge of the subsurface layers (for detailed discussion see Gough 1995).

To carry out the inversions we used optimally localized averaging (e.g., Gough, 1996; also Däppen *et al.*, 1991); to estimate  $\delta u$  at radius  $r_0$ , we construct a linear combination of the relative differences,

$$\sum c_i(r_0) \frac{\delta \nu_i}{\nu_i} = \frac{\int \left( \sum c_i K_{u,\gamma_1}^i \right) \frac{\delta u}{u} dr + \int \left( \sum c_i K_{\gamma_1,u}^i \right) \frac{\delta \gamma_1}{\gamma_1} dr}{\sum c_i \frac{F(\nu_i)}{I_i}} \quad (2)$$



*Figure 3.* The relative difference in the squared isothermal sound speed between the sun and the reference model (Christensen-Dalsgaard *et al.*1996), inferred from the LOI+LOWL frequencies for the two sets. (Left) For set A: the lower curve represented by 4 points was obtained by excluding  $l = 0, n = 15$  from the inversion; at greater values of  $r/R_{\odot}$  the removal of the datum hardly influences the inversions. (Right) For set B: inversion without the correlation matrix; its inclusion barely affected the inversion.

in such a way that it provides an estimate of a localized average of  $\delta u$  in the vicinity of  $r = r_0$  without undue contamination by  $\delta\gamma_1$  and by the errors in the data. Specifically, we choose the coefficients  $c_i$  that minimize

$$S \equiv \int K_{u,\gamma_1}(r, r_0)^2 (r - r_0)^2 dr + \alpha \int K_{\gamma_1,u}(r, r_0)^2 dr + \beta \sum_{i,j} c_i c_j E_{ij} \quad (3)$$

where  $E_{ij}$  is the covariance matrix between the uncertainties in the frequencies. Expression (3) is minimized subject to

$$\int K_{u,\gamma_1} dr = 1 \quad (4)$$

and

$$\sum_i c_i \frac{P_{\lambda}(\nu_i)}{I_i} = 0 \quad , \quad \lambda = 0, \dots, \lambda_{\max} \quad , \quad (5)$$

where

$$K_{u,\gamma_1}(r, r_0) \equiv \sum_i c_i K_{u,\gamma_1}^i(r) \quad , \quad (6)$$

$$K_{\gamma_1,u}(r, r_0) \equiv \sum_i c_i K_{\gamma_1,u}^i(r) \quad (7)$$

are the averaging kernel for  $u$  and the kernel determining the contamination by  $\delta\gamma_1$  of the inference, and  $P_{\lambda}(\nu_i)$  is a Legendre polynomial.

The first term in  $S$  encourages localization of the averaging kernel, which has unit modulus imposed by the first constraint; the second suppresses the

amplitude of the contaminating kernel, and the third suppresses error magnification and the correlation between the frequencies. Thus the parameters  $\alpha$  and  $\beta$  are used to balance the weights between resolution, contamination from  $\delta\gamma_1$ , and error. The purpose of the second set of constraints is to eliminate the contribution from the unknown surface layers, with a resolution determined by the value of  $\lambda_{\max}$  in the Legendre decomposition of  $F(\nu_i)$ .

Owing to the small number of LOI modes, the degree of localization is not very good. To obtain a better localization, it is essential to supplement the dataset with higher-degree modes. We used the LOWL dataset (Tomczyk *et al.* 1996) for this purpose. From the LOWL 2-year average dataset, 1013 modes with  $l \geq 8$  in the frequency range  $1.5\text{MHz} \leq \nu \leq 3.5\text{MHz}$  were chosen and added to the LOI frequencies. The improved averaging kernels obtained from the combined dataset are shown for set A in Fig. 2, which illustrates the importance of having higher-degree modes. Fig. 3 (Left) shows the result of the inversion for set A, together with a result of a second inversion, where we excluded a single mode ( $l = 0, n = 15$ ) because a problem with that mode was recognized during the analysis. We note how sensitive our inference of the deepest part of the sun can be to just a single mode. Fig. 3 (Right) shows the result of the inversion of set B.

There seem to be systematic differences between the LOWL and the LOI frequencies, which have a noticeable influence on the results of the inversion. We have confirmed that this does not result principally from the correlation between the uncertainties in the low-degree frequencies by carrying out an inversion with mode set B in which the off-diagonal components of  $E_{ij}$  were ignored: the results were superficially similar. However, we suspect that the fact that the LOWL and the LOI data were accumulated in different time intervals is significant; in addition the instruments observe in velocity and in intensity, respectively. The influence of the surface uncertainties is known to vary with time over the solar cycle, and to assume that the function  $F(\nu_i)$  in equation (1) is the same for both the LOWL and the LOI data is therefore inconsistent. A discrepancy of this kind caused by temporal variations of the surface layers can be manifest in the inversions as an error in the structure of the core.

#### 4. Conclusion

We have carried out a more careful analysis of the LOI p-mode frequencies than that which we reported previously (Fröhlich *et al.*, 1997) with no significant effect on the results of inversion. If there are any systematic errors in the analysis of the spectra, a yet more careful analysis will be required to remove them. We must point out that the improved treatment of the spectra is yet to be performed for  $l \geq 4$ . As a result of fitting the power

spectra, the frequency correlation matrix might have been underestimated. We acknowledge that systematic errors could play a very important role in the inferences of the internal solar structure. Nevertheless, we can conclude that the fine details of the spherically averaged structure of the solar core is unlikely to be very different from the latest standard solar model.

### Acknowledgements

The VIRGO team is led by Claus Fröhlich (PMOD/WRC, CH) and includes the following co-investigators (in alphabetical order): Bo Andersen, Thierry Appourchaux, Gabrielle Berthomieu, Dominique Crommelynck, Werner Däppen, Vicente Domingo, Alain Fichot, Douglas Gough, Todd Hoeksema, Antonio Jiménez, Judit Pap, Janine Provost, Teodoro Roca Cortés, José Romero, Thierry Toutain, Christoph Wehrli, Richard Willson.

We are grateful to Laurent Gizon on commenting an earlier version of the paper. Many thanks to S.Tomczyk and J.Schou for providing the LOWL data through the web.

### References

- Appourchaux, T., Andersen, B.N., Fröhlich, C., Jiménez, A., Telljohan, U., Wehrli, C. (1997) Submitted to *Solar Phys.*
- Appourchaux, T., Telljohann, U., Martin, D., Lévêque, S. and Fleur, J. (1995a) in *Fourth SOHO workshop on helioseismology*, V.Domingo and T.Hoeksema eds., ESA SP-376, p. 359
- Appourchaux, T., Toutain, T., Telljohann, U., Jiménez, A., Rabello-Soares, M.C., Andersen, B.N. and Jones, A.R. (1995b) *Astron. Astrophys.*, **294**, L13
- Appourchaux, T., Toutain, T., Telljohann, U., Jiménez, A., Rabello-Soares, M.C., Andersen, B.N. and Jones, A.R. (1995c) in *Fourth SOHO workshop on helioseismology*, V.Domingo and T.Hoeksema eds., ESA SP-376, p. 265
- Christensen-Dalsgaard *et al.* (1996) *Science*, **272**, 1286
- Däppen, W., Gough, D.O., Kosovichev, A.G. and Thompson, M.J. (1991) in *Challenges to Theories of the Structure of Moderate-Mass Stars*, Gough, D.O. & Toomre, J. eds., Springer Verlag, Berlin, p. 111
- Fröhlich, C. and the VIRGO team (1997) Submitted to *Solar Phys*
- Gough, D.O. (1995) in *Fourth SOHO workshop on helioseismology*, V. Domingo and T.Hoeksema eds., ESA SP-376, p. 249
- Gough, D.O. (1996) in *The structure of the Sun*, T. Roca Cortés & F. Sánchez eds., Cambridge University Press, p 141
- Rabello-Soares, M.C. (1996) Helioseismological study of the solar interior, PhD thesis, Universidad de La Laguna: La Laguna, Tenerife, Spain
- Rabello-Soares, M.C., Roca-Cortes, T., Jiménez, A., Appourchaux, T. and Eff-Darwich. (1996) Submitted to *Astrophys. J*
- Schou, J. (1992) On the analysis of helioseismic data, PhD Thesis, Aarhus University: Aarhus, Denmark
- Tomczyk, S., Schou, J. and Thompson, M.J. (1996) *Astrophys. J.*, **448**, L57